Regional Elemental Abundances within South Pole-Aitken Basin as Measured with Lunar Prospector Gamma-ray Spectrometer Data. D. J. Lawrence[1], C. M. Pieters[2], R. C. Elphic[1], W. C. Feldman[1], O. Gasnault[3], S. Maurice[3], and T. H. Prettyman[1], [1]Los Alamos National Laboratory, Los Alamos, NM, USA, 87545 (djlawrence@lanl.gov); [2]Brown University, Providence, RI, USA; [3]Observatoire Midi-Pyrénées, Toulouse France.

Introduction: South Pole-Aitken (SPA) basin is one of the largest impact basins in the solar system [1] and is a target of intense study since it is thought that SPA basin excavated deep into the lunar crust and possibly even the mantle [2,3,4]. These conclusions are supported by the observed mafic and thorium composition anomalies seen across the entire basin [5,6,7]. One of the major goals of lunar and planetary science [8] has been to measure and understand the composition of the non-mare materials within SPA basin. It is expected that this information will help to increase our understanding of the formation and differentiation processes that occurred early on the Moon.

We now have information from a fully reduced Lunar Prospector Gamma-ray Spectrometer (LP-GRS) dataset [9] so we can evaluate the broad compositional differences within SPA basin. Here we present the results of a study where we have examined the abundances for both mare and non-mare materials within SPA basin using the LP-GRS data. In addition, we compare these results to the abundances that are seen in the anorthositic highlands to the north of SPA basin.

Data Selection and analysis: For this study, we are using the following data: FeO [10] and Th [11] abundances are taken from the low-altitude (30km) portion of the LP mission and mapped onto 0.5°x0.5° pixels (15km x 15km at the equator); Al_2O_3, FeO and MgO abundances are taken from the high-altitude (100km) portion of the LP mission and mapped onto 150km x 150km pixels [9].

Our study area (80°S–20°S, 140°E–240°E) is shown in Figs. 1 and 2. Our initial selection is to define SPA basin as being all locations in the study area having an elevation of less than –2.5 km using Clementine topography data [12]. The contours in Figs. 1 and 2 show the SPA boundary as selected. In order to select mare regions, we used geologic maps [13,14] that have been digitized onto 0.5°x0.5° pixels, as shown by the red regions in Fig. 1. Finally, to make sure the measurements of non-mare materials are not contaminated by mare materials because of footprint spreading [11,15], we have masked out all locations that are closer than 90km to a mare unit but still within the SPA contour (blue regions in Fig. 1).

Results: Figs. 3 – 5 show example results from the low-altitude FeO and Th data as well as the high-altitude MgO data. For all of these figures, we have plotted histograms where selections have been made for the different units. The black line in all plots shows the abundance distribution for the entire basin; the red line shows the distribution for mapped mare units; the blue line shows the distribution for non-mare units outside the footprint mask (i.e., between the blue regions in Fig. 1 and the SPA contour); finally, the green line shows the abundance distribution for an anorthositic highlands region north of SPA basin (20°S–40°N, 160°E–260°E). This region was shifted 20° to the east to avoid the high-iron region of Mare Moscoviense.

FeO abundances: We can make a number of conclusions regarding the FeO data of Fig. 3. First, we see a clear difference between the mare and non-mare units within SPA basin. In particular, the mare data show higher average abundances than the non-mare regions. While the absolute mare abundances (10–11 FeO wt.%) are significantly lower than typical mare basalts of the near side, these low values are likely due to footprint mixing of lower-iron non-mare regions into the relatively small mare basalt regions. The non-mare abundances have measured abundances of 8–9 FeO wt.%. Finally, all of SPA basin shows higher FeO abundances than the anorthositic highlands, which have abundances in the range of 4.5–5 FeO wt.%.

Th abundances: As with the FeO data, the Th data (Fig. 4) also show differences between the mare and non-mare units. The mare regions show abundances ranging from 1.5 – 2.5 μg/g. This is similar to some of the abundances seen in some nearside, eastern mare basalts. The non-mare distribution appears to show two components. One is a low-thorium component (~1 μg/g) that is found both around Apollo basin and in the southern-most part of SPA basin. A somewhat higher abundance component (~1.5–2.5 μg/g) appears to be indistinguishable from the mare distribution. Finally, as with the FeO data, the thorium abundances also show higher values within SPA basin compared to the selected highlands region.

MgO abundances: With the high-altitude, large footprint data of [9], we might have questioned whether the mare and non-mare units could be distinguished within SPA basin. However, the MgO, as well as the high-altitude FeO and Al_2O_3 (not shown) data all showed compositional differences between the two units. Fig. 5 shows the results for MgO. While the histogram bins are by necessity larger than the previous plots (due to the fewer number of pixels), differences between the mare and non-mare distributions are nonetheless observed. Specifically, the mare distribution shows generally higher abundances (10–12 MgO wt.%)

compared to the non-mare units (7–10 MgO wt.%). Furthermore, all of SPA basin has higher abundances than the highlands region to the north.

Conclusions: Geochemical analysis of the SPA region would benefit from further analysis of footprint mixing either through forward modeling [11] of the GRS data, spatial deconvolution, or both. Nevertheless, even with this initial analysis, we find we are able to compositionally characterize and discriminate the non-mare and mare materials within SPA basin and compare them to local highlands. These geochemical data illustrate the unusual composition of the basin interior. The data are also consistent with the mineralogical interpretations of Clementine data that characterize the SPA non-mare material as noritic breccias derived from the lower crust or mantle after removal of the anorthositic upper crust [4].

References: [1] Spudis, et al., *Science*, 266, 1848, 1994; [2] Pieters, et al., *Geophys. Res. Lett.*, 24, 1903, 1997; [3] Lucey et al., *J. Geophys. Res.*, 105, 3701, 1998; [4] Pieters, et al., *J. Geophys. Res.*, 106(#E11), 28001, 2001; [5] Belton, et al., *Science*, 255, 570, 1992; [6] Lucey et al., *Science*, 266, 1855, 1994; [7] Lawrence et al., Science, 281, 1484, 1998; [8] Solar System Exploration Survey, Space Studies Board, National Research Council, 2002; [9] Prettyman et al., *The Moon Beyond 2002*, Abstract #3069; [10] Lawrence et al., J. Geophys. Res., 107, 10.1029/2001JE001530, 2002; [11] Lawrence et al., Met. Planet. Sci., in preparation, 2003; [12] Smith et al., *J. Geophys. Res.*, 102, 1591, 1997; [13] Stuart-Alexander, USGS I-1047, 1978; [14] Wilhelms et al., USGS I-1162, 1979. [15] Gasnault et al., *33rd LPSC*, Abstract #2010, 2002;

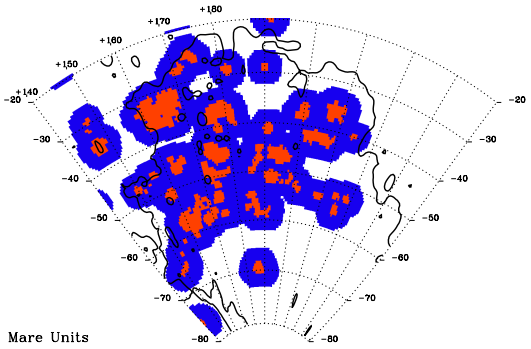

Figure 1. Mapped mare basalt units (red) and regions located ≤90km from mare basalt units (blue). The selected SPA contour is shown in black.

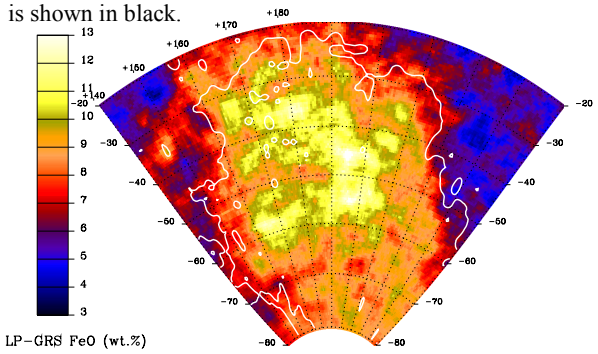

Figure 2. LP-GRS FeO abundances in and around SPA basin. The selected contour of SPA basin is shown in white.

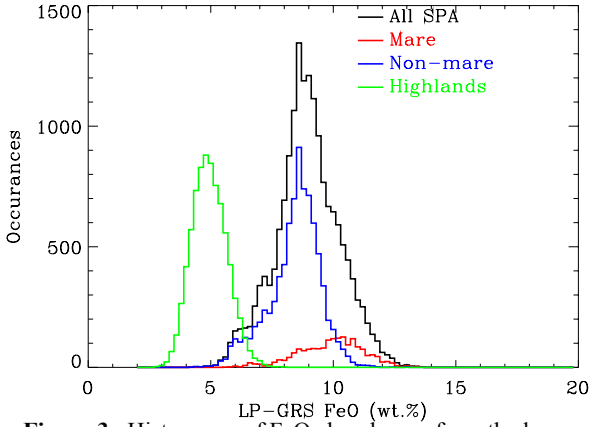

Figure 3. Histograms of FeO abundances from the low-altitude, 0.5°x0.5° data.

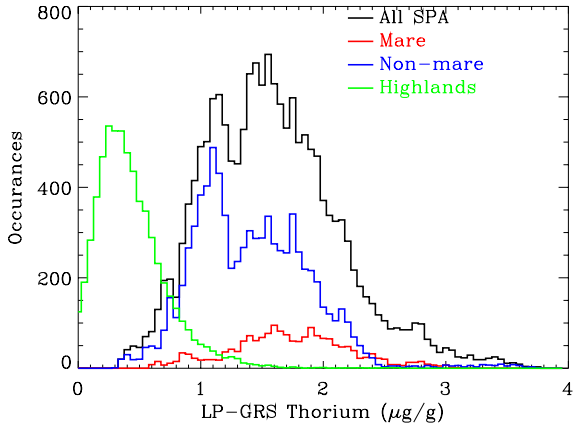

Figure 4. Histograms of Th abundances from the low-altitude, 0.5°x0.5° data.

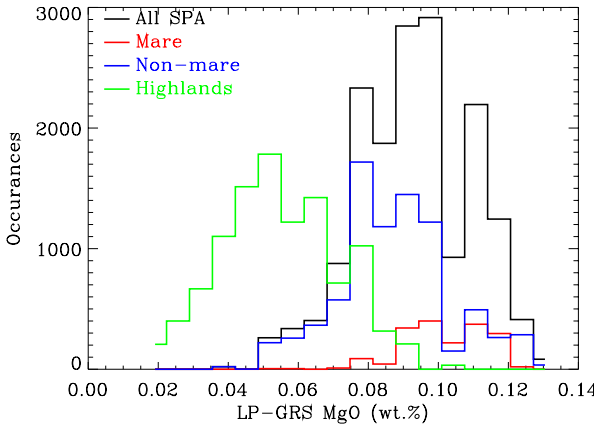

Figure 5. Histograms of MgO abundances from the high-altitude, 150km x 150km data.